

Supporting Information

Synthesis and Characterization of Quinoxaline-Fused Cyclopenta[*cd*]azulene

Tomohiro Oda ¹, Yuina Onishi ¹, Akihito Konishi ^{1,2,*}, and Makoto Yasuda ^{1,2,*}

¹ Department of Applied Chemistry, Graduate School of Engineering, Osaka University, 2-1 Yamadaoka, Suita, Osaka 565-0871, Japan; a-koni@chem.eng.osaka-u.ac.jp (A.K.), and yasuda@chem.eng.osaka-u.ac.jp (M.Y.)

² Innovative Catalysis Science Division, Institute for Open and Transdisciplinary Research Initiatives (ICS-OTRI), Osaka University, Suita, Osaka 565-0871, Japan; a-koni@chem.eng.osaka-u.ac.jp (A.K.), and yasuda@chem.eng.osaka-u.ac.jp (M.Y.)

* Correspondence: a-koni@chem.eng.osaka-u.ac.jp (A.K.), and yasuda@chem.eng.osaka-u.ac.jp (M.Y.) ; Tel.: +81-6-6879-7384

Table of contents

1. General	3
2. Materials.....	3
3. Synthetic procedures	4
4. X-ray crystallographic data	14
4-1. Summary for crystallographic data of 4.....	14
4-2. Summary for crystallographic data of 4Me ⁺ ·I ⁻	15
5. Electronic absorption spectra	16
6. Electrochemical properties	16
7. Computational method.....	17
7-1. General	17
7-2. Molecular orbitals for 4, 5, and 4Me ⁺	17
7-3. TD-DFT calculations for 4, 5, and 4Me ⁺	19
7-4. Cartesian coordinates for the optimized geometries	21
8. References.....	22

1. General

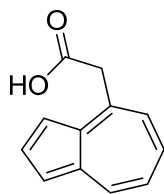
NMR spectra were recorded on a JEOL-ECS400 spectrometer (400 MHz for ^1H and 100 MHz for ^{13}C). The ^1H and ^{13}C NMR signals of compounds were assigned using HMQC, HSQC, HMBC, COSY, and ^{13}C off-resonance techniques. Positive FAB, EI, MALDI-TOF mass spectra were recorded on JEOL JMS-700, Shimadzu GCMS-QP2010 Ultra, and JEOL JMS-S3000 instruments, respectively. High-resolution DART and ESI mass spectra were measured using a JEOL JMS-T100LP spectrometer. IR spectra were recorded on a JASCO FT/IR 6200 spectrophotometer using thin films or KBr pellets. UV-vis-NIR spectra were recorded on a JASCO V-770 spectrophotometer. Cyclic voltammetry (CV) measurements were performed with an ALS-600C electrochemical analyzer using a glassy carbon working electrode, a Pt counter electrode, and an Ag/AgNO₃ reference electrode at room temperature in THF containing 0.1 M $n\text{Bu}_4\text{NClO}_4$ as the supporting electrolyte. Data collection for X-ray crystal analysis was performed on a Rigaku/XtaLAB Synergy-S/Cu diffractometer ($\text{CuK}\alpha$ $\lambda = 1.54187 \text{ \AA}$). All nonhydrogen atoms were refined with anisotropic displacement parameters and hydrogen atoms were placed at calculated positions and refined riding on their corresponding carbon atoms using the Olex2 program.[1]

2. Materials

Anhydrous dichloromethane, THF, acetonitrile, diethyl ether, toluene, hexane, and all reagents were obtained from commercial suppliers and used as received. Pristine azulene was purchased from commercial sources. 4-Methylazulene **7** was synthesized from azulene according to reported procedures.[2,3] Compound **5** was synthesized as a reference following a reported method.[4]

3. Synthetic procedures

2-(Azulen-4-yl)acetic acid **8**

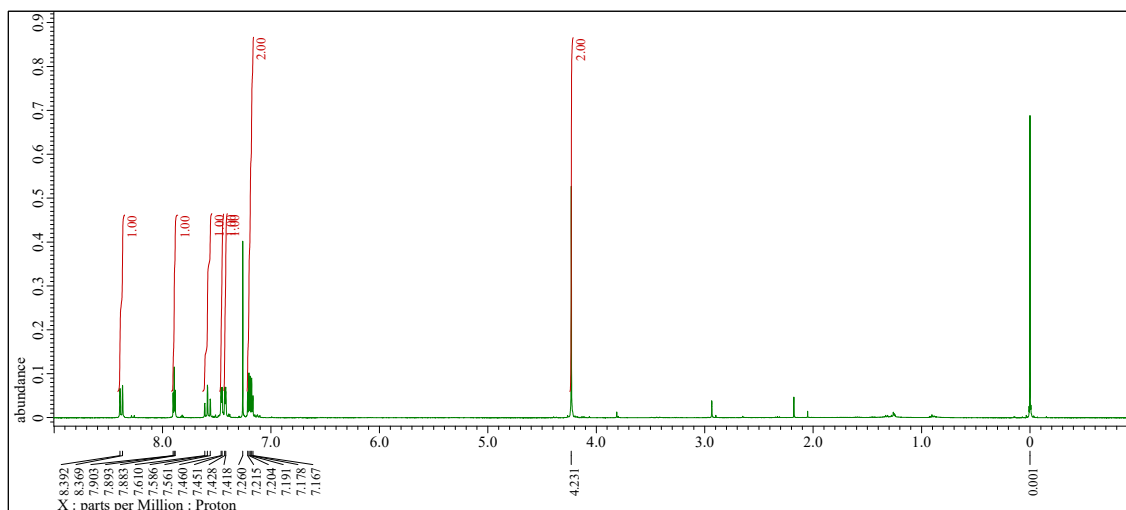


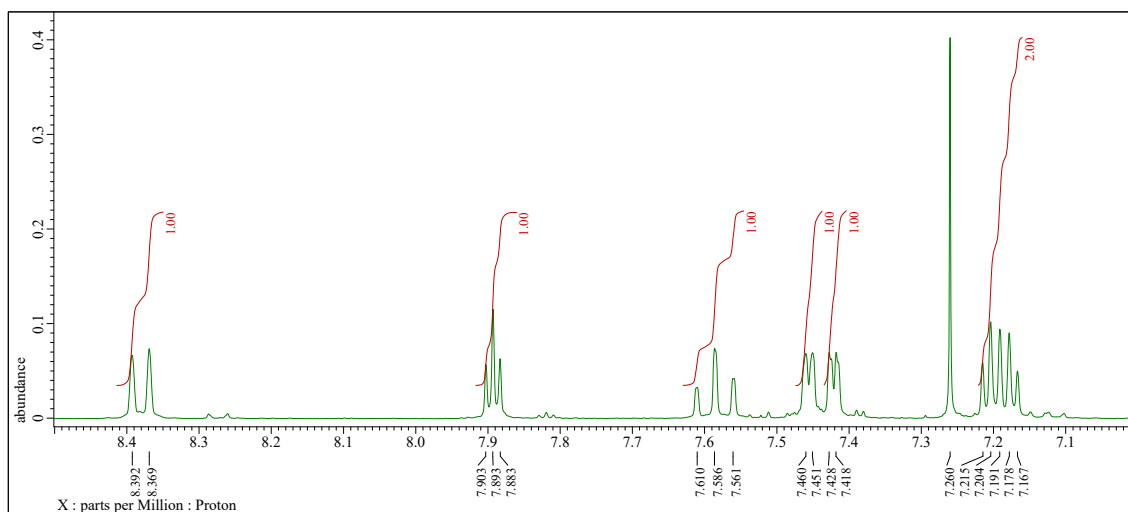
8

Under nitrogen atmosphere, to a solution of diisopropylamine (4.64 mL, 42.2 mmol) in dried THF (12 mL) was added *n*BuLi (26.4 mL, 70.3 mmol, 2.66 M in hexane solution) at 0 °C and the reaction mixture was stirred for 15 min. To a solution of 4-methylazulene **7** (4.00g, 28.1 mmol) in dried THF (75 mL) was added the prepared THF solution of LDA at -78 °C and the reaction mixture was stirred for 1 h at the temperature. Gaseous carbon dioxide was vigorously bubbled into the solution for 5 min at -78 °C. The reaction was quenched by aqueous HCl (2 M). The products were extracted with Et₂O and the organic layer was washed with saturated aqueous NaHCO₃ solution. The obtained water layer was acidified with aqueous HCl (2 M) and extracted with Et₂O. The filtrate was washed with water and dried over Na₂SO₄. After filtration, the obtained solution was evaporated under vacuum to give **8** as a blue solid (4.62 g, 24.8 mmol, 88%).

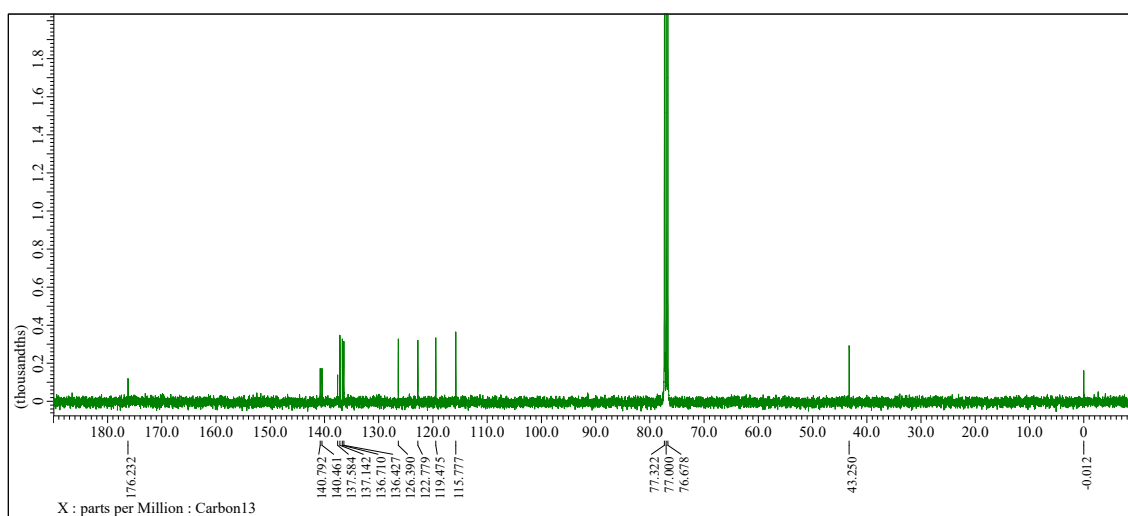
mp 122.2–123.0 °C; IR (KBr) ν = 3075 (s), 3009 (s), 2959 (s), 2922 (s), 2638 (m), 2532 (m), 1686 (s), 1562 (s), 1486 (m), 1442 (s), 1393 (s), 1363 (s), 1323 (m), 1267 (s), 1226 (s), 1186 (m), 1070 (w), 1025 (w), 953 (m), 761 (s) cm⁻¹; ¹H NMR (400 MHz, CDCl₃) 8.38 (d, *J* = 9.2 Hz, 1H), 7.89 (t, *J* = 4.0 Hz, 1H), 7.59 (t, *J* = 9.6 Hz, 1H), 7.46 (d, *J* = 3.6 Hz, 1H), 7.42 (d, *J* = 4.0, 1H), 7.19 (t, *J* = 9.6 Hz, 1H), 7.19 (d, *J* = 10.4 Hz, 1H), 4.23 (s, 2H); ¹³C{¹H} NMR (100 MHz, CDCl₃); 176.2, 140.8, 140.5, 137.6, 137.1, 136.7, 136.4, 126.4, 122.8, 119.5, 115.8, 43.3; HRMS (DART⁺) Calculated (C₁₂H₁₁O₂): 187.0754 ([M+H]⁺), Found: 187.0758.

¹H NMR: (400 MHz, CDCl₃)

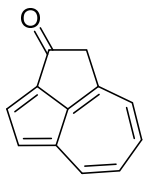




¹³C{¹H} NMR: (100 MHz, CDCl₃)



Cyclopenta[*cd*]azulen-2(1*H*)-one **9**

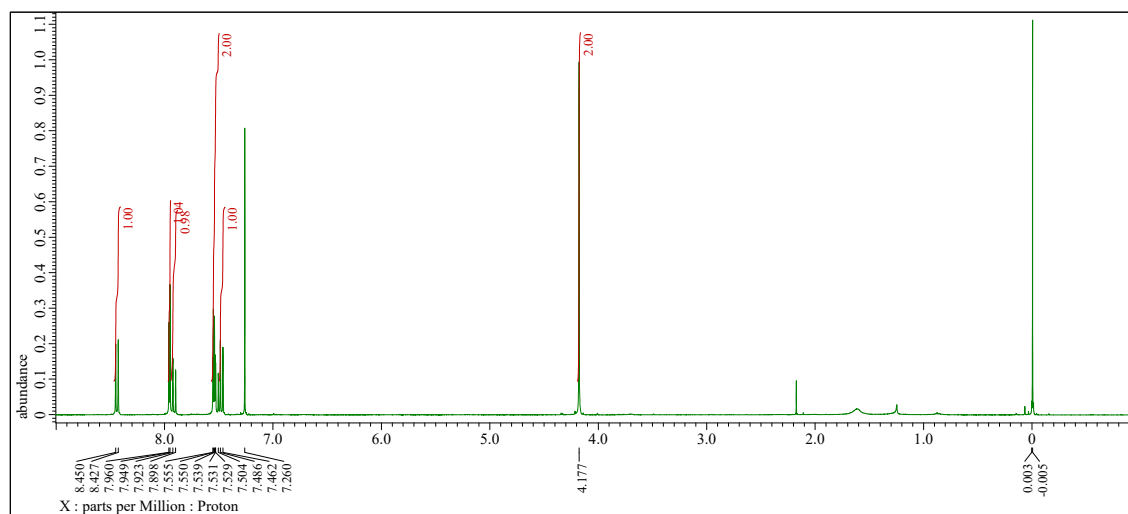


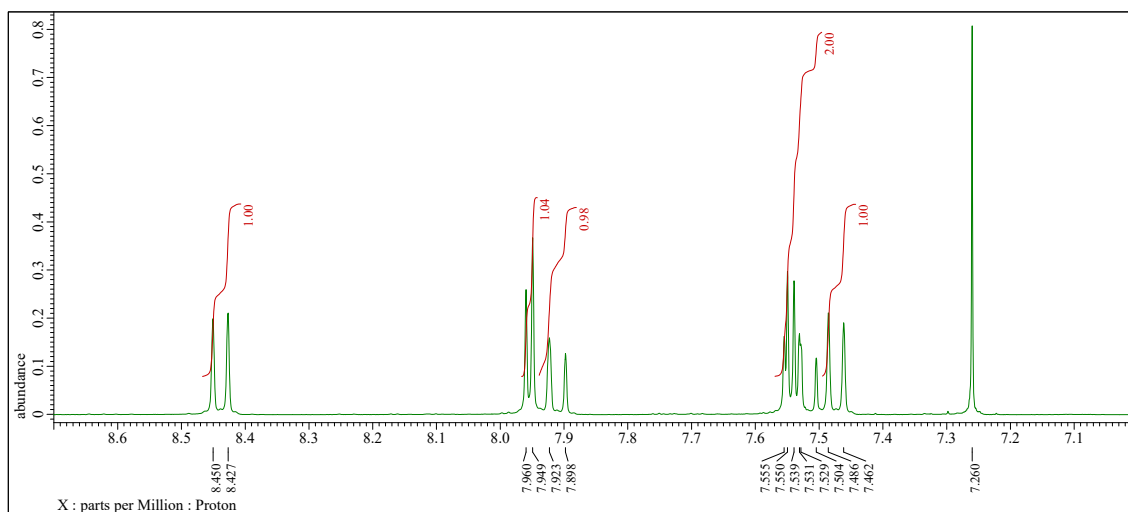
9

Under nitrogen atmosphere, to a solution of **8** (2.67 g, 14.3 mmol) in dried THF (65 mL) was added acetic anhydride (9.5 mL) and dried pyridine (19.5 mL) at room temperature. After the reaction mixture was stirred for 2 h, the reaction was quenched by aqueous HCl (2 M). The products were extracted with EtOAc. The organic layer was washed with saturated aqueous NaHCO₃ and water and dried over Na₂SO₄. After filtration, the obtained solution was evaporated under vacuum. The residues were purified by column chromatography on silica gel with hexane and ethyl acetate (60:40) to give **9** as a purple solid (818 mg, 4.87 mmol, 34%).

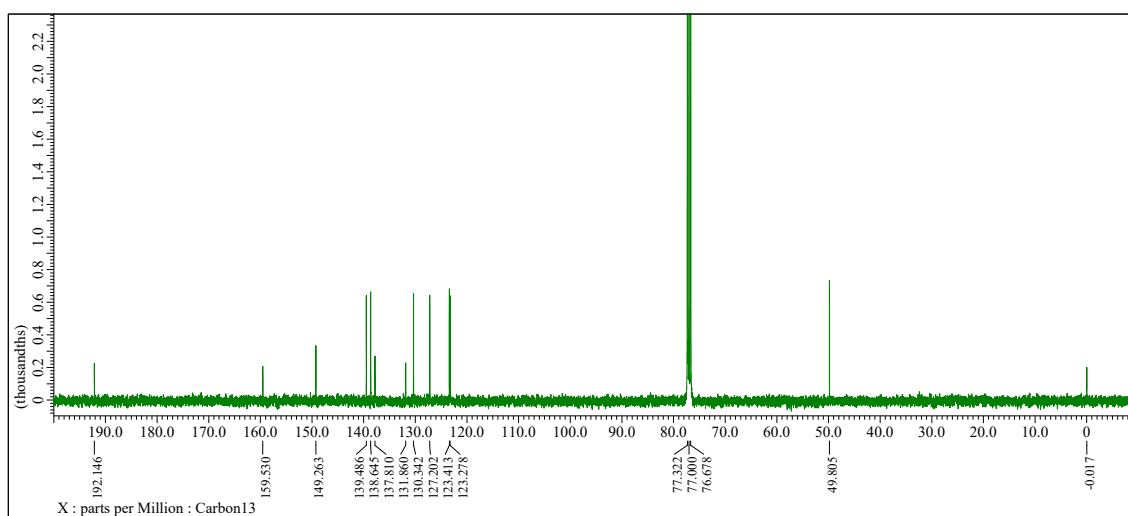
mp 104.5–105.4 °C; IR (KBr) ν = 3060 (m), 2928 (m), 2293 (w), 1771 (w), 1659 (s), 1589 (s), 1450 (s), 1384 (s), 1327 (s), 1265 (s), 1236 (s), 1202 (s), 1140 (m), 1015 (s), 959 (s), 930 (m), 841 (m), 795 (s), 739 (s) cm⁻¹; ¹H NMR (400 MHz, CDCl₃) 8.44 (d, *J* = 9.2 Hz, 1H), 7.95 (d, *J* = 4.4 Hz, 1H), 7.92 (t, *J* = 10.0 Hz, 1H), 7.54 (d, *J* = 4.4 Hz, 1H), 7.53 (dd, *J* = 10.2, 9.8 Hz, 1H), 4.18 (s, 2H); ¹³C{¹H} NMR (100 MHz, CDCl₃) 192.1, 159.5, 149.3, 139.5, 138.6, 137.8, 131.9, 130.3, 127.2, 123.4, 123.3, 49.8; HRMS (DART⁺) Calculated (C₁₂H₉O): 169.0648 ([M+H]⁺), Found: 169.0647.

¹H NMR: (400 MHz, CDCl₃)

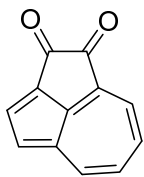




$^{13}\text{C}\{^1\text{H}\}$ NMR: (100 MHz, CDCl_3)



Cyclopenta[cd]azulene-1,2-dione **6**

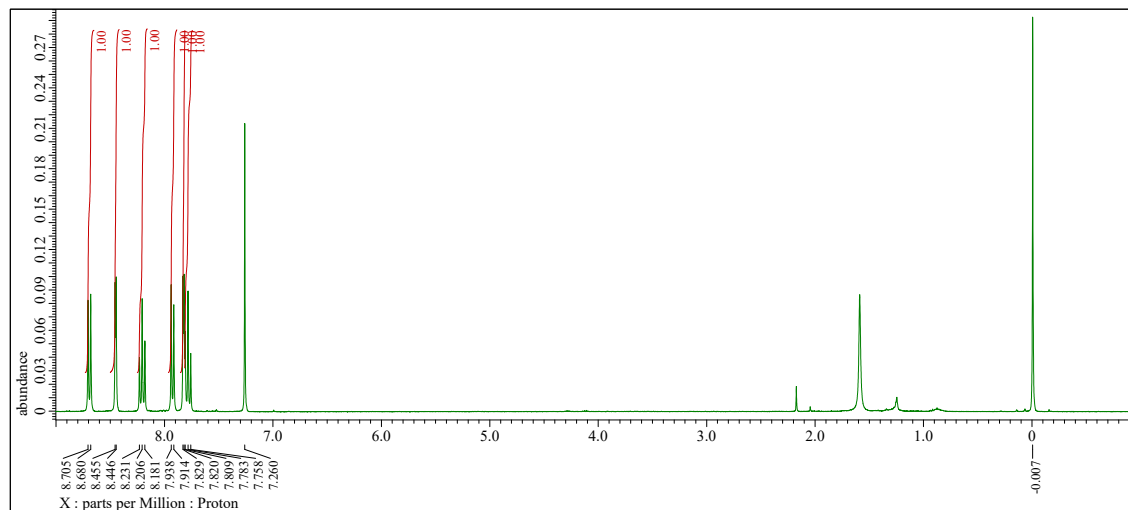


6

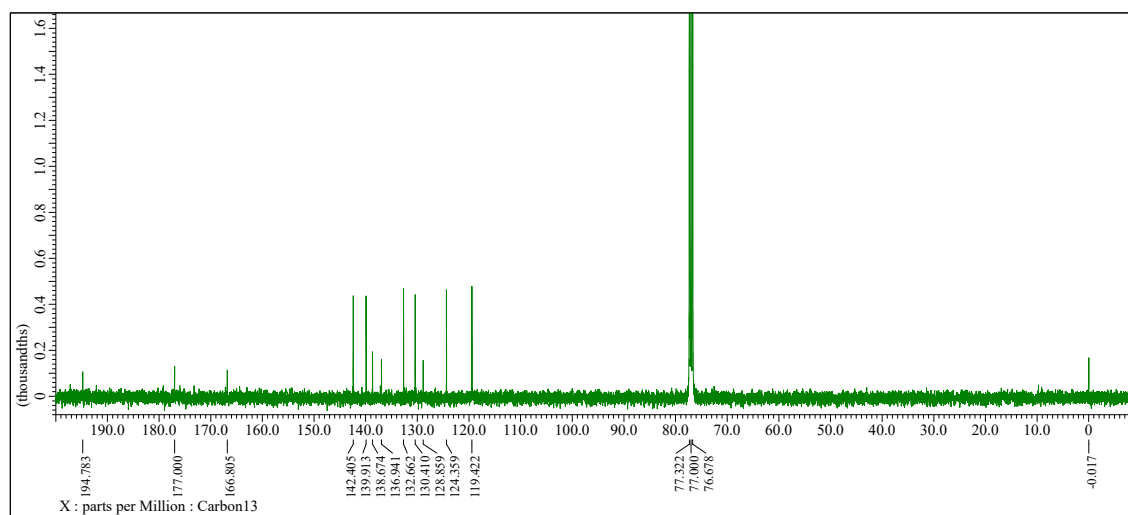
Under nitrogen atmosphere, to a solution of **9** (39.1 mg, 0.233 mmol) in dried DMF (2.3 mL) was added selenium dioxide (57.4 mg, 0.517 mmol) at room temperature and the reaction mixture was stirred for 4 h at 55 °C. The residue was removed by filtration through a celite pad. The products were extracted with EtOAc. The organic layer was washed with water and dried over Na₂SO₄. After filtration, the obtained solution was evaporated under vacuum. The residue was purified by column chromatography on silica gel (hexane: EtOAc = 50:50) to give **6** as a green solid (31.5 mg, 0.173 mmol, 75%).

mp >300 °C; IR (KBr) ν = 3077 (w), 3036 (w), 2985 (w), 2359 (w), 1871 (w), 1739 (s), 1691 (s), 1605 (s), 1549 (m), 1454 (w), 1436 (w), 1399 (s), 1333 (s), 1297 (m), 1223 (m), 1148 (w), 995 (w), 813 (m), 741 (m) cm⁻¹; ¹H NMR (400 MHz, CDCl₃) 8.69 (d, J = 10.0 Hz, 1H), 8.45 (d, J = 3.6 Hz, 1H), 8.21 (t, J = 10.0 Hz, 1H), 7.93 (d, J = 9.6 Hz, 1H), 7.82 (d, J = 3.6 Hz, 1H), 7.78 (t, J = 10.0 Hz, 1H); ¹³C{¹H} NMR (100 MHz, CDCl₃) 194.8, 177.0, 166.8, 142.4, 139.9, 138.7, 136.9, 132.7, 130.4, 128.9, 124.4, 119.4; HRMS (DART⁺) Calculated (C₁₂H₇O₂): 183.0441 ([M+H]⁺), Found: 183.0442.

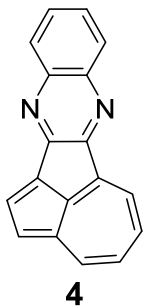
¹H NMR: (400 MHz, CDCl₃)



$^{13}\text{C}\{^1\text{H}\}$ NMR: (100 MHz, CDCl_3)



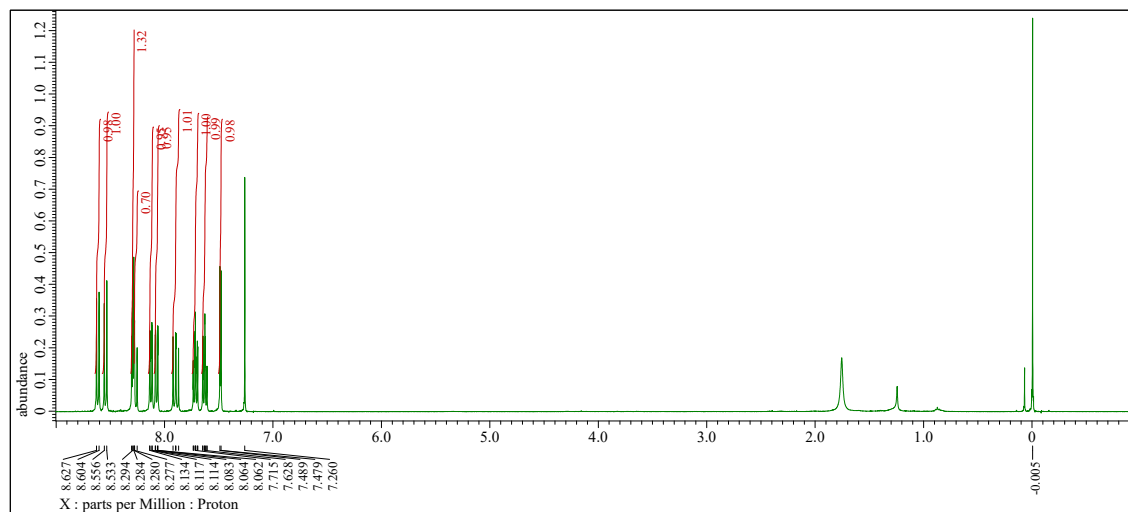
Cyclopenta[3,4]azuleno[1,2-*b*]quinoxaline **4**

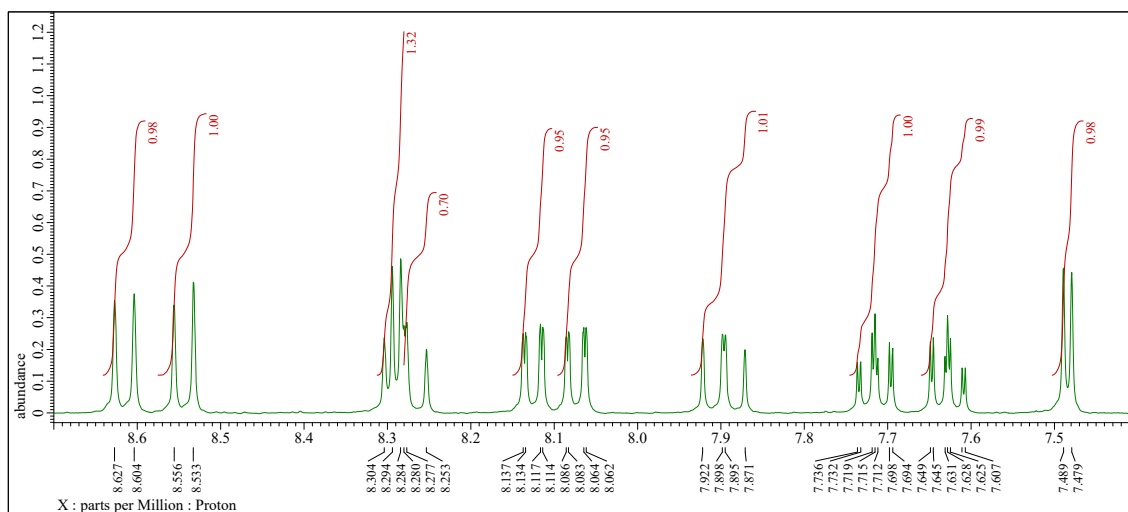


Under nitrogen atmosphere, to a solution of **6** (31.5 mg, 0.169 mmol) and LiCl (0.72 mg, 0.017 mmol) in dried EtOH (10 mL) was added 1,2-phenylenediamine (25.4 mg, 0.235 mmol) at room temperature and the reaction mixture was stirred for 2 h. The products were extracted with CHCl₃. The organic layer was washed with water and dried over Na₂SO₄. After filtration, the solvent was removed under vacuum. The residue was purified by column chromatography on silica gel (hexane: EtOAc = 60:40) to give **4** as a green solid (39.9 mg, 0.157 mmol, 96%).

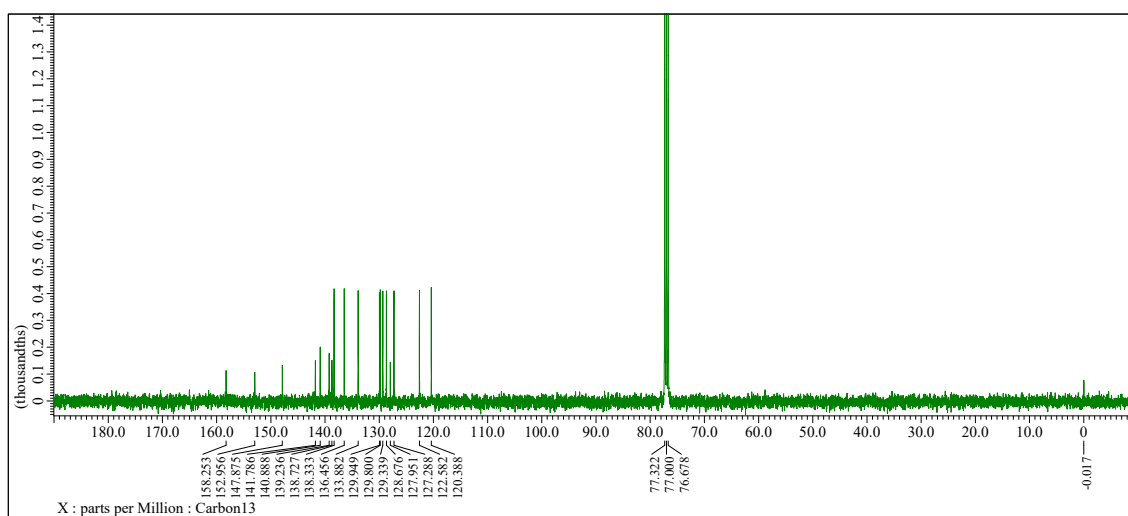
mp 218.1–218.9 °C; IR (KBr) ν = 3090 (w), 3047 (w), 1602 (m), 1563 (s), 1516 (m), 1437 (s), 1335 (m), 1296 (m), 1237 (m), 1081 (m), 981 (w), 795 (s), 764 (s), 742 (s) cm⁻¹; ¹H NMR (400 MHz, CDCl₃) 8.62 (d, *J* = 9.2 Hz, 1H), 8.54 (d, *J* = 9.2 Hz, 1H), 8.29 (d, *J* = 4.0 Hz, 1H), 8.28 (dd, *J* = 10.8, 9.6 Hz, 1H), 8.13 (dd, *J* = 8.0, 1.2 Hz, 1H), 8.07 (d, *J* = 8.8, 1.2 Hz, 1H), 7.90 (dd, *J* = 10.8, 9.6 Hz, 1H), 7.72 (ddd, *J* = 8.4, 6.8, 1.6 Hz, 1H), 7.63 (ddd, *J* = 8.4, 7.0, 1.6 Hz, 1H), 7.48 (d, *J* = 4.0 Hz, 1H); ¹³C{¹H} NMR (100 MHz, CDCl₃) 158.3, 153.0, 147.9, 141.8, 140.9, 139.2, 138.7, 138.3, 136.5, 133.9, 129.9, 129.8, 129.3, 128.7, 127.9, 127.3, 122.6, 120.4; HRMS (DART⁺) Calculated (C₁₈H₁₁N₂): 255.0917 ([M+H]⁺), Found: 255.0925.

¹H NMR: (400 MHz, CDCl₃)

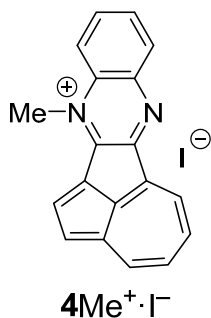




$^{13}\text{C}\{^1\text{H}\}$ NMR: (100 MHz, CDCl_3)



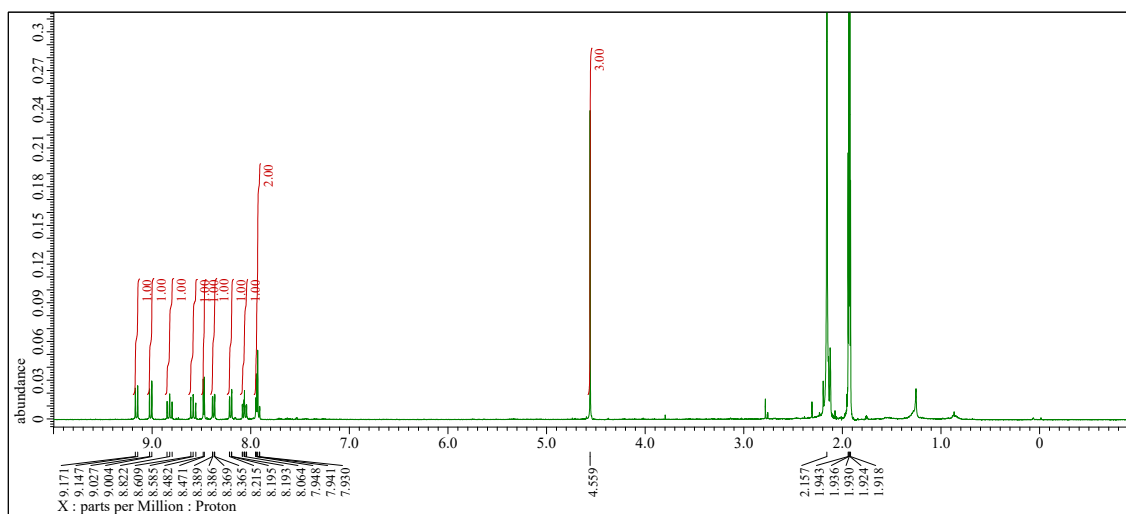
***N*-methylation: 12-Methylcyclopenta[3,4]azuleno[1,2-*b*]quinoxalin-12-ium iodide 4Me⁺·I⁻**

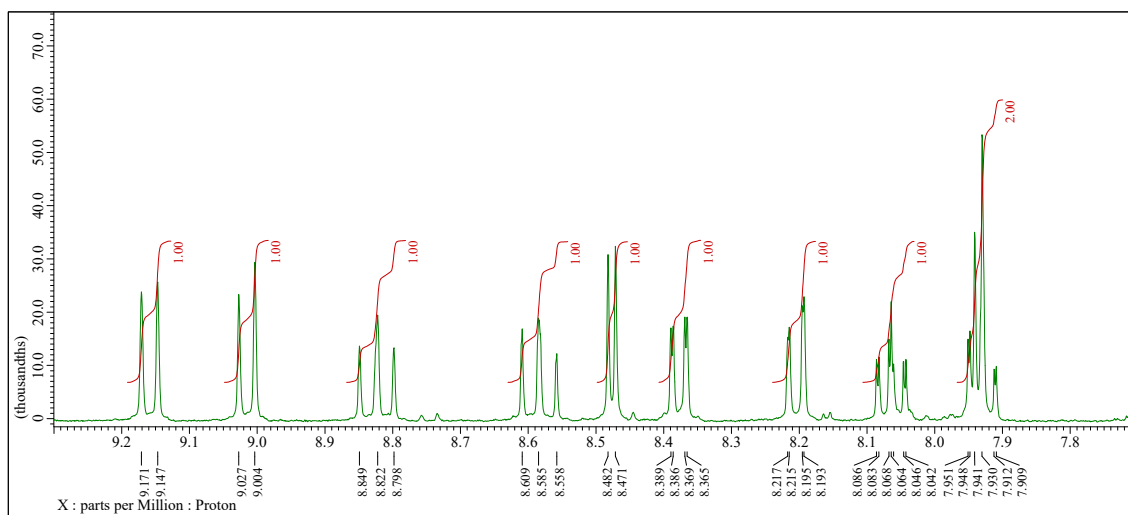


Under nitrogen atmosphere, to a solution of **4** (24.9 mg, 0.0980 mmol) in acetonitrile (15 mL) was added iodomethane (609 mg, 4.29 mmol) at room temperature. The reaction mixture was stirred for 14 h at 80 °C and the solvent was removed in vacuum, to give **4Me⁺·I⁻** as a dark brown solid (33.4 mg, 0.0843 mmol, 86%). The low solubility in common organic solvents hampered recording the ¹³C NMR spectrum.

mp 253.1–254.0 °C; IR (KBr) ν = 3036 (m), 2958 (m), 1943 (w), 1856 (w), 1746 (w), 1671 (w), 1622 (s), 1587 (s), 1534 (m), 1488 (s), 1452 (m), 1419 (s), 1393 (s), 1348 (s), 1251 (m), 1092 (m), 1052 (m), 817 (s), 765 (s) cm⁻¹; ¹H NMR (400 MHz, CD₃CN) 9.16 (d, J = 9.6 Hz, 1H), 9.02 (d, J = 9.2 Hz, 1H), 8.82 (t, J = 10.2 Hz, 1H), 8.59 (t, J = 10.2 Hz, 1H), 8.48 (d, J = 4.4 Hz, 1H), 8.38 (dd, J = 8.2, 1.4 Hz, 1H), 8.21 (dd, J = 8.8, 0.8 Hz, 1H), 8.06 (ddd, J = 8.8, 7.4, 1.4 Hz, 1H), 7.95–7.91 (m, 2H), 4.56 (s, 3H); HRMS (MALDI-TOF MS), Calculated (C₁₉H₁₃N₂): 269.1073 ([M-I]⁺), Found: 269.1044.

¹H NMR: (400 MHz, CD₃CN)





4. X-ray crystallographic data

4-1. Summary for crystallographic data of 4

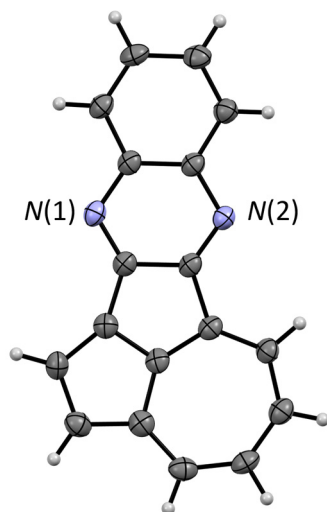


Figure S1. Molecular structure of **4** in the crystalline state measured at 123 K.

No. CCDC	2414718	From a CHCl ₃ /AcOEt solution	
Empirical Formula	C ₁₈ H ₁₀ N ₂	<i>Z</i> value	4
Formula Weight	254.28	<i>D</i> _{calc} / g·cm ⁻³	1.419
Crystal Color, Habit	dark green, needle	<i>F</i> ₀₀₀	528.0
Crystal Dimensions / mm	0.08 × 0.04 × 0.02	μ (CuK α) / mm ⁻¹	0.662
Crystal System	orthorhombic	Data/restraints/parameters	1963/0/181
Space Group	<i>P</i> 2 ₁ 2 ₁ 2 ₁ (#19)	Residuals: <i>R</i> 1	0.0472
<i>a</i> / Å	4.9303(2)	(<i>I</i> > 2.00 σ (<i>I</i>))	
<i>b</i> / Å	14.0494(6)	Residuals: <i>wR</i> 2	0.1328
<i>c</i> / Å	14.0494(6)	(<i>all data</i>)	
α / °	90	Goodness of Fit Indicator	1.119
β / °	90		
γ / °	90		
Volume / Å ³	1190.23(9)		
Temperature / K	123		

4-2. Summary for crystallographic data of 4Me⁺·I⁻

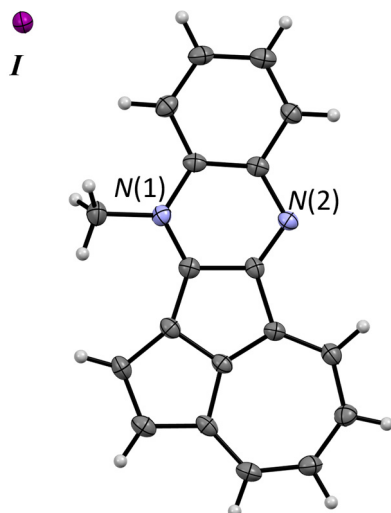


Figure S2. Molecular structure of 4Me⁺·I⁻ in the crystalline state measured at 123 K.

No. CCDC	2414719	From an acetonitrile solution	
Empirical Formula	C ₁₉ H ₁₃ IN ₂	<i>Z</i> value	2
Formula Weight	396.21	<i>D</i> _{calc} / g·cm ⁻³	1.750
Crystal Color, Habit	pale pink, block	<i>F</i> ₀₀₀	388.0
Crystal Dimensions / mm	0.13 × 0.08 × 0.06	<i>μ</i> (CuK α) / mm ⁻¹	16.689
Crystal System	triclinic	Data/restraints/parameters	3055/0/200
Space Group	<i>P</i> -1 (#2)	Residuals: <i>R</i> 1	0.0298
<i>a</i> / Å	7.2958(2)	(<i>I</i> > 2.00 σ (<i>I</i>))	
<i>b</i> / Å	9.5609(2)	Residuals: <i>wR</i> 2	0.0789
<i>c</i> / Å	11.0014(2)	(<i>all data</i>)	
α / °	82.376(2)	Goodness of Fit Indicator	1.098
β / °	81.441(2)		
γ / °	89.213(2)		
Volume / Å ³	752.13(3)		
Temperature / K	123		

5. Electronic absorption spectra

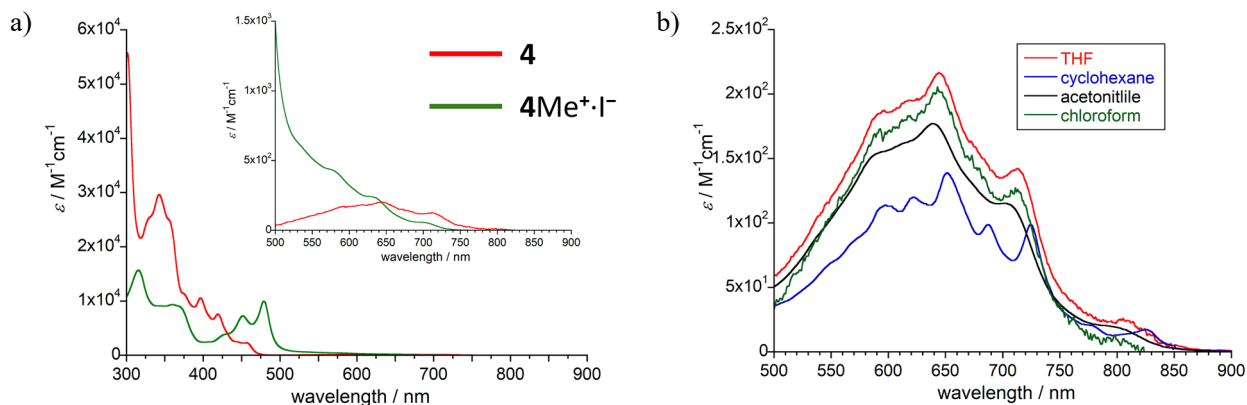


Figure S3. (a) Electronic-absorption spectra of **4** and $4\text{Me}^+\cdot\text{I}^-$ in CHCl_3 .

4: λ / nm ($\epsilon / \text{M}^{-1}\text{cm}^{-1}$): 711 (127), 643 (206), 593 (173), 456 (2300), 419 (7600), 396 (10600), 343 (29600), 301 (55800).

$4\text{Me}^+\cdot\text{I}^-$: λ / nm ($\epsilon / \text{M}^{-1}\text{cm}^{-1}$): 699 (58), 634 (236), 580 (426), 479 (9980), 451 (7250), 427 (3800), 360 (9340), 315 (15700).

(b) Expanded electronic-absorption spectra of **4** in various solvents.

6. Electrochemical properties

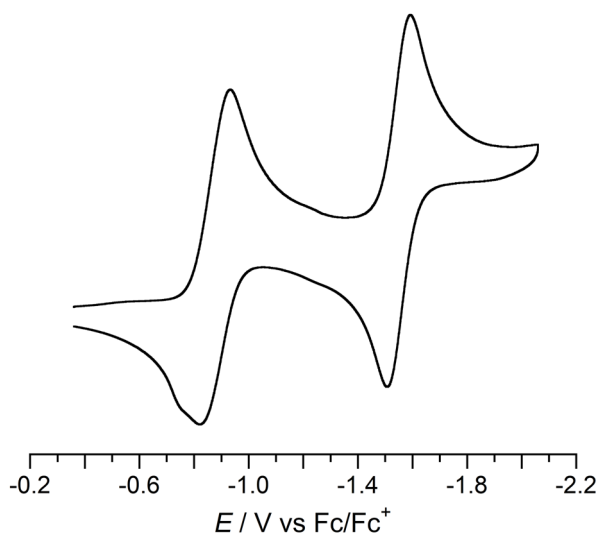


Figure S4. Cyclic voltammogram (CV) of $4\text{Me}^+\cdot\text{I}^-$ (V vs. Fc/Fc^+ , in 0.1M $n\text{Bu}_4\text{NClO}_4$ /acetonitrile, scan rate = 100 mV/s, room temperature).

7. Computational method

7-1. General

All quantum chemical calculations were conducted using the Gaussian 16 Rev. C. 01 program.[5] The geometries of neutral singlet species of **4**, **5**, and 4Me^+ were optimized with the B3LYP-D3 functional and 6-311G* basis set. From the frequency analyses, the calculated geometries of **4**, **5**, and 4Me^+ locate at the local minimum giving all positive vibrational frequencies. The obtained B3LYP-D3 geometries were employed for the calculations of the other physical properties.

Symmetry-adapted molecular orbitals were evaluated at the B3LYP/6-311+G* level. NICS(1) values were calculated at the GIAO-B3LYP/6-311+G* method using the optimized structure. AICD plots for **4** and 4Me^+ were calculated by using the method developed by Herges[6] and only π -electrons are considered at the CSGT-B3LYP/6-311+G*//B3LYP-D3/6-311G* level. Yellow surface is the isosurface of the induced current density under the magnetic field. Green arrows with red head indicate the induced current density vectors. The clockwise and counterclockwise density vectors indicate diamagnetic and paramagnetic ring currents, respectively.

Electronic excitation properties for **4**, **5**, and 4Me^+ were evaluated by the TDDFT method with B3LYP and 6-311+G* basis set.

7-2. Molecular orbitals for **4**, **5**, and 4Me^+

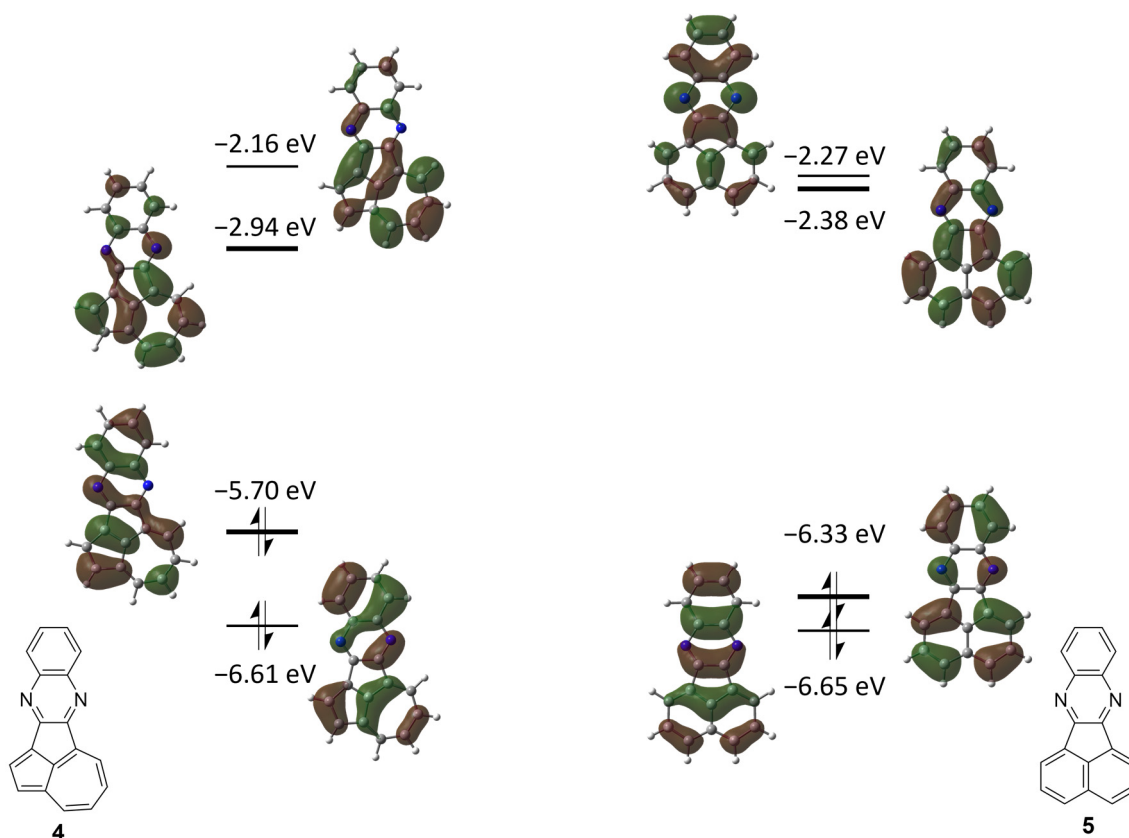


Figure S5. Calculated orbital energy diagram of HOMO-1, HOMO, LUMO, LUMO+1 for **4** and **5** at the B3LYP/6-311+G*//B3LYP-D3/6-311G* level.

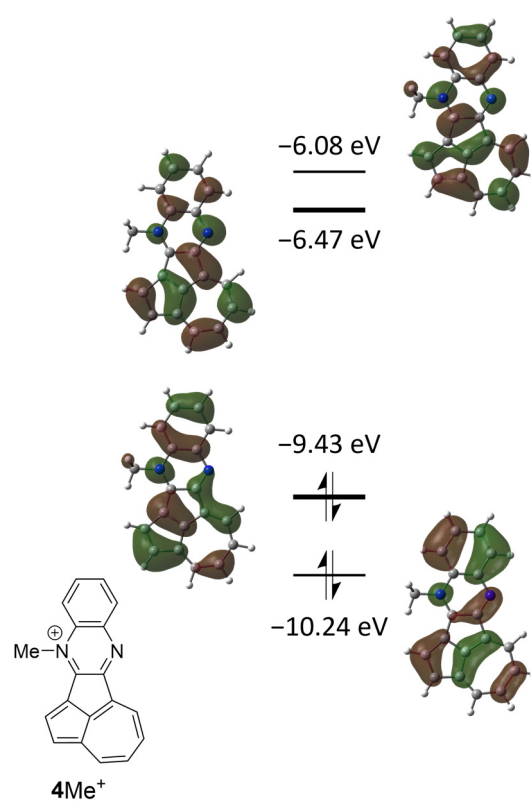


Figure S6. Calculated orbital energy diagram of HOMO-1, HOMO, LUMO, LUMO+1 for 4Me^+ at the B3LYP/6-311+G**/B3LYP-D3/6-311G* level.

7-3. TD-DFT calculations for **4**, **5**, and **4Me⁺**

Table S1. Excitation energies of **4** calculated at the TD-B3LYP/6-311+G**/B3LYP-D3/6-311G* level.

Excited state number	Excitation energy / eV (wavelength / nm)	Excitation amplitudes	Oscillator strength
1	1.94 (638)	0.700 (HOMO – LUMO)	0.0007
2	3.00 (413)	–0.146 (HOMO–4 – LUMO) –0.223 (HOMO–3 – LUMO) 0.644 (HOMO – LUMO+1)	0.0257
3	3.04 (408)	0.695 (HOMO–2 – LUMO)	0.0003
4	3.11 (400)	0.563 (HOMO–1 – LUMO) 0.408 (HOMO – LUMO+2)	0.0127
5	3.55 (350)	–0.301 (HOMO–4 – LUMO) 0.484 (HOMO–3 – LUMO) –0.245 (HOMO–1 – LUMO) 0.303 (HOMO – LUMO+2)	0.0561
6	3.61 (344)	–0.105 (HOMO–4 – LUMO+1) 0.325 (HOMO–3 – LUMO) 0.272 (HOMO–1 – LUMO) 0.374 (HOMO–1 – LUMO+1) 0.141 (HOMO – LUMO+1) –0.366 (HOMO – LUMO+2)	0.2815

Table S2. Excitation energies of **5** calculated at the TD-B3LYP/6-311+G**/B3LYP-D3/6-311G* level.

Excited state number	Excitation energy / eV (wavelength / nm)	Excitation amplitudes	Oscillator strength
1	3.46 (359)	–0.329 (HOMO–1 – LUMO+1) 0.614 (HOMO – LUMO)	0.0512
2	3.48 (356)	0.134 (HOMO–4 – LUMO) 0.370 (HOMO–1 – LUMO) 0.582 (HOMO – LUMO+1)	0.0000
3	3.50 (354)	0.703 (HOMO–2 – LUMO+1)	0.0017
4	3.60 (344)	0.589 (HOMO–1 – LUMO) –0.373 (HOMO – LUMO+1)	0.0023
5	3.65 (340)	0.702 (HOMO–2 – LUMO)	0.0000
6	4.06 (305)	–0.334 (HOMO–3 – LUMO) 0.511 (HOMO–1 – LUMO+1) 0.320 (HOMO – LUMO)	0.7839

Table S3. Excitation energies of 4Me^+ calculated at the TD-B3LYP/6-311+G**/B3LYP-D3/6-311G* level.

Excited state number	Excitation energy / eV (wavelength / nm)	Excitation amplitudes	Oscillator strength
1	2.23 (555)	-0.134 (HOMO – LUMO+1) 0.684 (HOMO – LUMO)	0.0022
2	2.87 (431)	0.311 (HOMO-1 – LUMO) 0.113 (HOMO – LUMO) 0.604 (HOMO – LUMO+1)	0.1271
3	3.29 (377)	-0.244 (HOMO-2 – LUMO) -0.319 (HOMO-1 – LUMO) 0.147 (HOMO – LUMO+1) 0.555 (HOMO – LUMO+2)	0.0164
4	3.46 (359)	0.175 (HOMO-2 – LUMO) 0.445 (HOMO-1 – LUMO) 0.394 (HOMO-1 – LUMO+1) -0.176 (HOMO – LUMO+1) 0.229 (HOMO-1 – LUMO+2)	0.1939
5	3.66 (338)	-0.239 (HOMO-3 – LUMO) -0.201 (HOMO-2 – LUMO+1) -0.200 (HOMO-1 – LUMO) 0.525 (HOMO-1 – LUMO+1) 0.134 (HOMO – LUMO+1) -0.236 (HOMO-2 – LUMO+2)	0.0866

7-4. Cartesian coordinates for the optimized geometries

Table S4. Optimized geometries for **4** in the singlet state optimized at the B3LYP-D3/6-311G* level.

Atom	X	Y	Z	Atom	X	Y	Z
C	0.00000000	0.57617300	0.00000000	C	-2.06506700	-3.28114700	0.00000000
C	-1.46329800	0.34198100	0.00000000	C	-4.51580100	-0.30374000	0.00000000
C	0.67731400	-0.72517700	0.00000000	H	-4.53290000	1.79111900	0.00000000
C	-1.59398100	-1.04739700	0.00000000	C	2.75736000	2.81363100	0.00000000
C	-2.49774300	1.26631800	0.00000000	H	0.05225100	-3.91962400	0.00000000
N	0.62139700	1.71569000	0.00000000	C	4.07469800	0.33615500	0.00000000
C	-0.37349600	-1.72746200	0.00000000	H	-4.76955300	-2.41066400	0.00000000
N	1.97937400	-0.83474700	0.00000000	H	-2.58472700	-4.23014000	0.00000000
C	-2.68882200	-2.00173800	0.00000000	H	-5.60026100	-0.23117500	0.00000000
C	-3.86042400	0.93654100	0.00000000	C	4.13465600	2.75901000	0.00000000
H	-2.22847600	2.31806600	0.00000000	H	2.22181400	3.75682500	0.00000000
C	1.99564800	1.62638200	0.00000000	C	4.79478900	1.51212300	0.00000000
C	-0.67072700	-3.11392900	0.00000000	H	4.56213300	-0.63252300	0.00000000
C	2.66336500	0.35859600	0.00000000	H	4.71508100	3.67564600	0.00000000
C	-4.02186100	-1.62040500	0.00000000	H	5.87959000	1.48037900	0.00000000

Table S5. Optimized geometries for **5** in the singlet state optimized at the B3LYP-D3/6-311G* level.

Atom	X	Y	Z	Atom	X	Y	Z
C	-0.00000000	0.72897588	-0.23111205	C	0.00000000	1.27770027	3.98225790
C	0.00000000	1.17749404	1.16809492	H	0.00000000	3.39381404	3.71615550
C	-0.00000000	-0.72897588	-0.23111205	C	-0.00000000	1.40454706	-3.72320501
C	0.00000000	-0.00000000	1.95535640	C	-0.00000000	-2.43038181	3.21666067
C	0.00000000	2.40149776	1.79680361	H	-0.00000000	-3.32413432	1.22684003
N	-0.00000000	1.44156229	-1.32342247	C	-0.00000000	-1.40454706	-3.72320501
C	-0.00000000	-1.17749404	1.16809492	H	0.00000000	-1.34770705	5.06586114
N	-0.00000000	-1.44156229	-1.32342247	H	0.00000000	1.34770705	5.06586114
C	0.00000000	-0.00000000	3.35848245	C	-0.00000000	0.70643445	-4.91001126
C	0.00000000	2.43038181	3.21666067	H	-0.00000000	2.48862982	-3.69596257
H	-0.00000000	3.32413432	1.22684003	H	-0.00000000	-3.39381404	3.71615550
C	-0.00000000	0.71693326	-2.48896782	C	-0.00000000	-0.70643445	-4.91001126
C	-0.00000000	-2.40149776	1.79680361	H	-0.00000000	-2.48862982	-3.69596257
C	-0.00000000	-0.71693326	-2.48896782	H	-0.00000000	1.24220472	-5.85357907
C	0.00000000	-1.27770027	3.98225790	H	-0.00000000	-1.24220472	-5.85357907

Table S6. Optimized geometries for **4Me⁺** in the singlet state optimized at the B3LYP-D3/6-311G* level.

Atom	X	Y	Z	Atom	X	Y	Z
C	0.00000000	0.70230900	0.00000000	H	-1.05620800	-3.13665300	0.00000000
C	-0.29859500	-0.73733700	0.00000000	C	-3.95047900	-0.46083400	0.00000000
C	1.47028800	0.85146600	0.00000000	C	2.96587200	-2.49694800	0.00000000
N	-1.58613100	-1.11076000	0.00000000	H	1.13398100	-3.68941500	0.00000000
C	0.92944800	-1.43996800	0.00000000	C	-3.19699200	2.24109200	0.00000000
N	-0.88421600	1.64029600	0.00000000	C	4.57716600	1.01451900	0.00000000
C	2.22702300	2.01288600	0.00000000	H	4.05737100	3.04628600	0.00000000
C	1.94954200	-0.45478100	0.00000000	C	4.43326700	-0.38187500	0.00000000
C	-1.95607300	-2.53311300	0.00000000	C	-4.90447100	0.54583400	0.00000000
C	-2.58990600	-0.12757600	0.00000000	H	-4.27555600	-1.49220600	0.00000000
C	1.59377100	-2.71042100	0.00000000	H	3.71872600	-3.27303600	0.00000000
C	-2.20322300	1.24584100	0.00000000	C	-4.53392900	1.89841200	0.00000000
C	3.62823200	2.04854400	0.00000000	H	-2.86960200	3.27378000	0.00000000
H	1.69541300	2.95911700	0.00000000	H	5.60692700	1.35927700	0.00000000
C	3.23469200	-1.08650500	0.00000000	H	5.35412500	-0.95868300	0.00000000
H	-2.53845900	-2.76426500	0.89204200	H	-5.95410800	0.27505400	0.00000000
H	-2.53845900	-2.76426500	-0.89204200	H	-5.29551600	2.66898600	0.00000000

8. References

1. Dolomanov, O. V.; Bourhis, L.J.; Gildea, R.J.; Howard, J.A.K.; Puschmann, H. OLEX2 : A Complete Structure Solution, Refinement and Analysis Program. *J. Appl. Crystallogr.* **2009**, *42*, 339–341, doi:10.1107/S0021889808042726.
2. Hafner, K.; Weldes, H. Zur Kenntnis Der Azulene II. Die Substitution Von Azulenene Mit Metallorganischen Verbindungen. *Justus Liebigs Ann. Chem.* **1957**, *606*, 90–99, doi:10.1002/jlac.19576060110.
3. Hatakenaka, R.; Nishikawa, N.; Mikata, Y.; Aoyama, H.; Yamashita, K.; Shiota, Y.; Yoshizawa, K.; Kawasaki, Y.; Tomooka, K.; Kamijo, S.; et al. Efficient Synthesis and Structural Analysis of Chiral 4,4'-Biazulene. *Chem. – A Eur. J.* **2024**, *202400098*, 1–9, doi:10.1002/chem.202400098.
4. Karami, B.; Rooydel, R.; Khodabakhshi, S. A Rapid Synthesis of Some 1,4-Aryldiazines by the Use of Lithium Chloride as an Effective Catalyst. *Acta Chim. Slov.* **2012**, *59*, 183–188.
5. Frisch, M.J.; Trucks, G.W.; Schlegel, H.B.; Scuseria, G.E.; Robb, M.A.; Cheeseman, J.R.; Scalmani, G.; Barone, V.; Petersson, G.A.; Nakatsuji, H.; et al. *Gaussian 16, Revision C.01*; Gaussian, Inc.: Wallingford CT, 2016;
6. Geuenich, D.; Hess, K.; Köhler, F.; Herges, R. Anisotropy of the Induced Current Density (ACID), a General Method To Quantify and Visualize Electronic Delocalization. *Chem. Rev.* **2005**, *105*, 3758–3772, doi:10.1021/cr0300901.